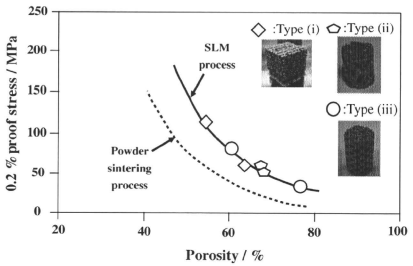

Fig. 6. Compressive strength of porous Ti metal with respect to porosity prepared by selective laser melting and compared with those prepared by a conventional powder sintering process.

and 20 μm on the density of the specimens was also examined, and the results showed similar densities of the final products in all cases.

Based on these results, a laser power of 117 W, scanning speed of 225 mm s^{-1}, hatch space of 90 μm, and hatch offset of 20 μm were used to fabricate porous bodies with a wall thickness of <1.8 mm.

3.2. Compressive strength of the porous specimens

The wall thicknesses of the various types of fabricated porous structures shown in Fig. 3 were in the range 400–800 μm. Cancellous bone structures consist of pores of different sizes ranging from 500 μm to 2 mm (Fig. 3i and ii), while the cubic structure has pores in the range 400–800 μm (Fig. 3iii). The compressive strengths of the various kinds of porous Ti metal fabricated by the SLM process is plotted against porosity in Fig. 6. The compressive strength was in the range 35–120 MPa when the porosities were in the range 75–55%. The results were compared with those of porous Ti metal prepared by the powder sintering method. The compressive strength of porous specimens fabricated by SLM was higher than that of those prepared by powder sintering, while the strength of specimens generated by both methods decreased with increasing porosity [3].

3.3. Surface structural changes on heat treatment

Fig. 7 shows the surface texture of the fabricated specimen, as well as of that subjected to heat treatment at 1300 °C in an argon gas atmosphere. Partially melted Ti particles were loosely bonded to the surface of the fabricated specimen. However, after heat treatment at 1300 °C, these particles were fused and bonded with the laser melted core part, producing a concave texture over the entire surface.

3.4. Surface structural changes in porous Ti metal on chemical and heat treatment and soaking in SBF

Fig. 8 shows FE-SEM photographs of a porous Ti metal that had been subjected to chemical and heat treatment after heat treatment at 1300 °C in an argon gas atmosphere. A fine network structure was formed on the surface of the porous Ti metal. These network structures were uniformly observed, even on the inner side of the pore.

Fig. 9 shows FE-SEM photographs of porous Ti metal soaked in SBF for 3 days after chemical and heat treatment. The walls of the porous body were completely covered with apatite after soaking in SBF for 3 days, indicating that the Ti metal surface had become bioactive after NaOH, HCl, and heat treatment.

3.5. In vivo bioactivity of the porous Ti metal

Gross inspection of the animal experiments showed that all rabbits tolerated the operative procedure well. No infection of the

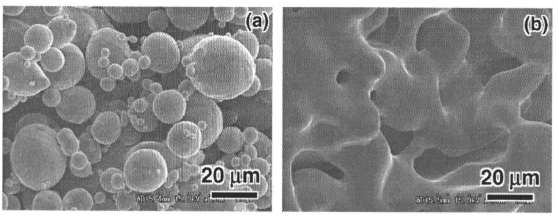

Fig. 7. FE-SEM photograph of the surface of porous Ti metal CBS (a) fabricated by SLM and (b) that heated at 1300 °C for 1 h in an argon gas atmosphere.

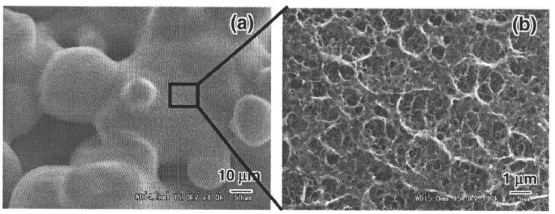

Fig. 8. FE-SEM photograph of porous Ti metal CBS subjected to NaOH, HCl and heat treatments after heat treatment at 1300 °C. (a) Low magnification; (b) high magnification showing fine network structure on the wall.

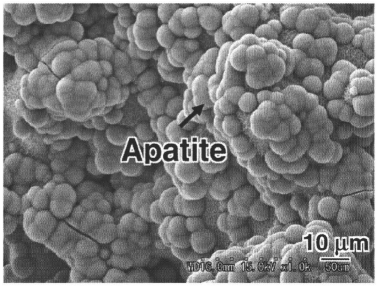

Fig. 9. Apatite particles formed on the surface of porous Ti metal CBS soaked in SBF for 3 days after NaOH, HCl and heat treatments.

operative site or dislocations of the implants were observed on dissection after death. All implanted porous Ti metal CBS and IPS specimens were stable and firmly bonded with the host bone at all post-implantation time points. No apparent adverse reactions, such as inflammation or foreign body reactions, were noted on or around any implanted samples by Stevenel's blue and Van Gieson's surface staining.

Within 3 weeks new bone was observed at the outer periphery and in the center of the chemical- and heat-treated specimens (results not shown). At the advancing bone front in the deep portion of the sample immature woven bone was found. There was no sign of cartilage formation or endochondral ossification. Marrow-like tissue formation was observed in the samples. Fig. 10 shows light microscope and SEM photographs of chemical- and heat-treated and untreated CBS samples 12 weeks after implantation. From Fig. 10 we can see that new bone was formed on the porous surface and bonded directly with the chemically treated layer. On the other hand, little new bone formation was observed on the surface of untreated implants. Fig. 11 shows a comparative histological study of porous Ti metal CBS and IPS samples subjected to chemical and heat treatment and implanted into the femurs of rabbits for 12 weeks. From Fig. 11 we can see that both CBS and IPS specimens showed mature bone strongly adhering to the porous wall. Fig. 12 shows the bone affinity indices (%) for chemical- and heat-treated CBS and IPS samples as well as for untreated samples for different implantation periods. The affinity indices of chemical- and heat-treated porous Ti metal CBS and IPS samples gradually increased with implantation period. There was a significant difference between the 52 week period and the other periods for the chemical- and heat-treated porous Ti metal CBS and IPS samples. After 12 and 52 weeks implantation the affinity indices of chemical- and heat-treated implants were significantly greater than those of the untreated implants.

4. Discussion

Using conventional fabrication techniques it is difficult to control the internal pore geometry, pore size, and distribution [3,34]. On the other hand, the SLM process is a useful technique to fabricate 3D porous structures directly from metallic powders and, hence, the process is suitable for the design of artificial bone substitutes with complex inner and outer geometries fitting the patient's defective bone. However, in this technique fine metal powders are melted by laser beam, which moves at a very high speed, and hence, this melting process may create internal defects due to some of the powder being blown off. In order to fabricate defect-free metallic implants it is important to optimize the power, scanning speed, and scanning pattern of the laser beam.

When the supplied energy density is insufficient to fully melt the powder, unmelted powder remains on the layer and produces defects. The temperature of the powder in the vicinity of the melted zone is low. In contrast, when the supplied energy density is sufficient to melt the powder, the melting zone becomes large and the temperature in the vicinity of the melted zone will remain high. This high temperature assists full melting of the powder in the next layer. Therefore, the density of the specimen depends

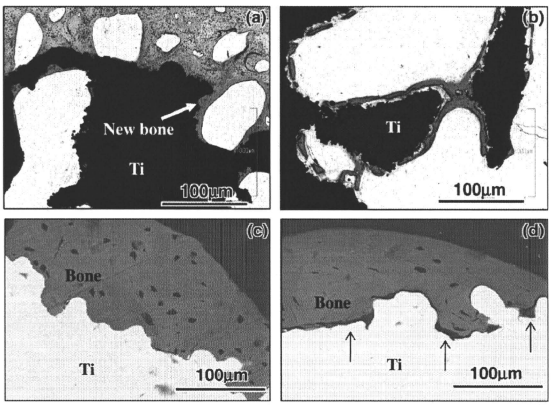

Fig. 10. Stevenel's blue and Van Gieson's surface staining of non-decalcified histological sections and SEM photographs of CBS samples after 12 weeks implantation. (a, c) Chemical- and heat-treated implants show new bone formation along the pore walls; (b, d) untreated implants show slight new bone formation along the pore walls. Red indicates bone. (For interpretation of the references to colour in this figure legend, the reader is referred to the web version of this article).

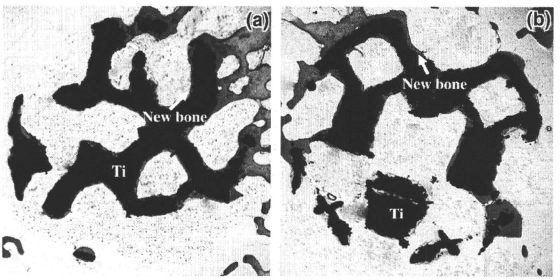

Fig. 11. Stevenel's blue and van Gieson's surface staining of non-decalcified histological section of chemical- and heat-treated porous Ti implants CBS and IPS after 12 weeks implantation in the femur of white rabbits.

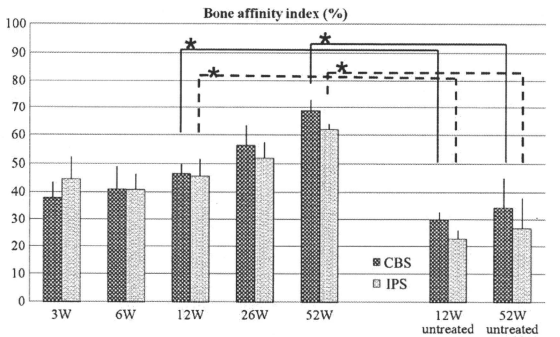

Fig. 12. Affinity indices (%) of the chemical- and heat-treated porous Ti implants CBS and IPS implanted in the femur of rabbit for different durations. The error bars are standard deviations. * Significant difference.

on the supplied energy density or on the ratio of laser power to scanning speed (P/V) at a constant thickness of powder layer. The critical value of P/V is approximately 0.5–0.6, as shown in Fig. 4. In general, both a boundary contour and a hatch beam are necessary to give an accurate shape and high density to the final product. However, similar trends in density as a function of P/V were observed when the specimens were fabricated using only a hatch beam, as shown in Fig. 4. As indicated in Fig. 5, the density of the thick plate specimen (>1.8 mm) does not depend on two consecutive hatch spaces. However, a large number of defects remained in the formed body when thin plate specimens (thinner than 1 mm) were fabricated with a hatch spacing of 180 μm, and their densities were low. A fully dense body with a thinner wall measuring 0.5 mm could be prepared by decreasing the space between the two consecutive hatch beams to 90 μm, as shown in Fig. 5. This suggests that two consecutive beams should be overlapped to fabricate thinner walls. When a laser beam scans to melt the powders to form a thin wall, the temperature is easily reduced by thermal conduction into the surrounding powder because of its small thermal capacity. This induces insufficient melting of the powder and the formation of internal defects. In the case of the fabrication of thick walls, the laser power is supplied over a wide zone, so the powder surrounding the melt zone remains hot for a longer time, which helps in melting of the Ti powder to reduce the defects and increase the density. If the hatch beam scanning interval is further reduced, defect formation can be avoided, because the energy supplied to the powder for each unit volume is sufficient to keep the temperature high in the melt zone.

In the present study we observed that large numbers of spherical Ti particles were partially bonded to the porous walls. In order to avoid release of these particles, the specimens were heated at 1300 °C in an argon gas atmosphere (Fig. 7). Although the mechanical strength might be decreased by the heat treatment [35], microcavities were formed on the wall, and these might be beneficial for interlock with the surrounding tissues when implanted in the living body. The compressive strength of the porous body processed by SLM was in the range 35–120 MPa when the volumetric porosities were in the range 75–55%. These values are higher than those of porous bodies prepared by the powder sintering method, as seen in Fig. 6. The improved compressive strength is attributed to the fine grain structure formed by rapid cooling of the laser melted body, whereas grain growth occurs during powder sintering. Further, the compressive strength of the porous body prepared by SLM might be little increased by the subsequent chemical and heat treatments [3].

Porous bodies prepared by the SLM process formed a fine uniform network structure on their pore walls after NaOH treatment, and these network structures remained stable even after subse-

quent HCl and heat treatment, as shown in Fig. 8. These network structures, as reported earlier, consist of anatase and rutile [25]. Chemical treatment has the advantage of uniform treatment, even within the pore. Porous bodies subjected to this chemical and heat treatment formed bone-like apatite on soaking in SBF within 3 days, as seen in Fig. 9. It has been believed that if a material forms a bone-like apatite layer on its surface in SBF it can induce direct bone formation through a similar apatite layer in the living body and bond to living bone [21,22]. In the present study similar results were verified in the animal experiments. As shown in Fig. 11, newly formed bone was observed on the periphery and in the center of both kinds of porous structures, CBS and IPS, within 12 weeks after implantation into the femurs of white rabbits. Porous CBS implants showed new bone formation (Fig. 10) in pores and bonded to the wall having nano-structured fine network structures due to previous NaOH, HCl, and heat treatments. On the other hand, untreated implants showed little bone formation in the pores. The amount of new bone on the surface of the untreated implants barely increased with time.

New bone on the surface of chemical- and heat-treated porous Ti metal CBS and IPS gradually increased with implantation time, compared with the untreated porous samples (Fig. 12). This indicates that the porous Ti metal fabricated by the SLM process has a high osteoconductive ability after subsequent NaOH, HCl, and heat treatments, the same as that of plasma sprayed porous Ti metal, as reported earlier [26,36]. Further detailed investigations on the influence of the porous structure on bone growth is in progress, and will be reported elsewhere.

The present study has shown that a porous structure consisting of thin-walled titanium metal with a structure similar to that of human cancellous bone could be prepared by the SLM process by optimizing the laser power, scanning speed, and hatching pattern. This SLM process could be useful to fabricate custom-made implants for biomedical applications tailored to the patient. Internal structure and porosity level can be easily controlled by the automated manufacturing process and, further, bioactivity can be provided by the subsequent chemical and heat treatments.

5. Conclusion

In order to fabricate a porous Ti metal with fully dense thin walls by a SLM process, laser power, scanning speed, and hatching pattern were optimized and various kind of porous bodies were fabricated. The compressive strength of the porous bodies prepared by SLM was found to be higher than that of a powder sintering process at the same level of porosity. Thus, the prepared porous structures analogous to human cancellous bone, when subjected to chemical and heat treatments, uniformly formed a fine network structure of titanium oxide layer, which formed bone-like apatite in SBF within 3 days. In vivo studies showed that newly formed bone was observed in the periphery and in the center of the chemical- and heat-treated cylindrical porous body within 12 weeks of implantation into the rabbit femoral condyle, and was directly bonded to the titanium wall. The SLM process has been found to be a useful technique for fabricating customized metallic implants with complicated internal structures, and the porous bodies thus fabricated are expected to be a useful bone substitutes after chemical and heat treatments.

Appendix A. Figures with essential colour discrimination

Certain figures in this article, particularly Figures 1–3, 6, 10 and 11 are difficult to interpret in black and white. The full colour images can be found in the on-line version, at doi:10.1016/j.actbio.2010.09.034.

References

[1] Ryan G, Pandit A, Apatsidis DP. Fabrication methods of porous metals for use in orthopaedic applications. Biomaterials 2006;27:2651–70.
[2] Wen CE, Yamada Y, Shimojima K, Chino Y, Hosokawa H, Mabuchi M. Novel titanium foam for bone tissue engineering. J Mater Res 2002;17:2633–9.
[3] Pattanayak DK, Matsushita T, Doi K, Takadama H, Nakamura T, Kokubo T. Effects of oxygen content of porous titanium metal on its apatite-forming ability and compressive strength. J Mater Sci Eng C 2009;29:1974–8.
[4] Das S, Wohlert M, Beaman JJ, Bourell DL. Processing of titanium net shapes by SLS/HIP. Mater Des 1999;20:115–21.
[5] Fischer P, Romano V, Weber HP, Karapatis NP, Boillat E, Glardon R. Sintering of commercially pure titanium powder with a Nd:YAG laser source. Acta Mater 2003;51:1651–62.
[6] Simchi A, Petzoldt F, Pohl H. On the development of direct metal laser sintering for rapid tooling. J. Mater Process Technol 2003;141:319–28.
[7] Williams JM et al. Bone tissue engineering using polycaprolactone scaffolds fabricated via selective laser sintering. Biomaterials 2005;26:4817–27.
[8] Santos EC, Shiomi M, Osakada K, Laoui T. Rapid manufacturing of metal components by laser forming. Int J Machine Tools Manuf 2006;46:1459–68.
[9] Traini T, Mangano C, Sammons RL, Mangano F, Macchi A, Piattelli A. Direct laser metal sintering as a new approach to fabrication of an isoelastic functionally graded material for manufacture of porous titanium dental implants. Dent Mater 2008;24:1525–33.
[10] Kumar S, Kruth JP. Composites by rapid prototyping technology. Mater Des 2010;31:850–6.
[11] Hollander DA, Walter MV, Wirtz T, Sellei R, Rohlfing BS, Paar O, et al. Structural, mechanical and in vitro characterization of individually structured Ti6Al4V produced by direct laser forming. Biomaterials 2006;27:955–63.
[12] Lin CY, Wirtz T, LaMarca F, Hollister SJ. Structural and mechanical evaluations of a topology optimized titanium interbody fusion cage fabricated by selective laser melting process. J Biomed Mater Res A 2007;83:272–9.
[13] Yadroitsev I, Bertrand Ph, Smurov I. Parametric analysis of the selective laser melting process. Appl Surf Sci 2007;253:8064–9.
[14] Mullen L, Stamp RC, Brooks WK, Jones E, Sutcliffe CJ. Selective laser melting: a regular unit cell approach for the manufacture of porous, titanium, bone ingrowth constructs, suitable for orthopedic applications. J Biomed Mater Res B Appl Biomater 2009;89:325–34.
[15] Mullen L, Stamp RC, Fox P, Jones E, Ngo C, Sutcliffe CJ. Selective laser melting: a unit cell approach for the manufacture of porous, titanium, bone in-growth constructs, suitable for orthopedic applications. II. Randomized structures. J Biomed Mater Res B Appl Biomater 2009;92:178–88.
[16] Hao L, Dadbakhsh S, Seaman O, Felstead M. Selective laser melting of a stainless steel and hydroxyapatite composite for load-bearing implant development. J Mater Process Technol 2009;209:5793–801.
[17] Stamp R, Fox P, Neill WO, Jones E, Sutcliffe C. The development of a scanning strategy for the manufacture of porous biomaterials by selective laser melting. J Mater Sci Mater Med 2009;20:1839–48.
[18] Thijs L, Verhaeghe F, Craeghs T, Humbeeck JV, Kruth JP. A study of the microstructural evolution during selective laser melting of Ti6Al4V. Acta Mater 2010;58:3303–12.
[19] Heinl P, Muller L, Korner C, Singer RF, Muller FA. Cellular Ti–6Al–4V structures with interconnected macro porosity for bone implants fabricated by selective electron beam melting. Acta Biomater 2008;4:1536–44.
[20] Hacking SA, Tanzer M, Harvey EJ, Krygier JJ, Bobyn JD. Relative contributions of chemistry and topography to the osseointegration of hydroxyapatite coatings. Clin Orthoped Rel Res 2002;405:24–38.
[21] Kim HM, Miyaji F, Kokubo T, Nakamura T. Preparation of bioactive Ti and its alloys via simple chemical surface treatment. J Biomed Mater Res 1996;32:409–17.
[22] Nishiguchi S, Fujibayashi S, Kim HM, Kokubo T, Nakamura T. Biology of alkali- and heat-treated titanium implants. J Biomed Mater Res A 2003;67:26–35.
[23] Fujibayashi S, Neo M, Kim HM, Kokubo T, Nakamura T. Osteoinduction of porous bioactive titanium metal. Biomaterials 2004;25:443–50.
[24] Kawanabe K et al. A new cementless total hip arthroplasty with bioactive titanium porous coating by alkaline and heat treatment: average 4.8 year results. J Biomed Mater Res B Appl Biomater 2009;90:476–81.
[25] Pattanayak DK, Kawai T, Matsushita T, Takadama H, Nakamura T, Kokubo T. Effect of HCl concentrations on apatite-forming ability of NaOH–HCl- and heat-treated titanium metal. J Mater Sci Mater Med 2009;20:1401–11.
[26] Takemoto M, Fujibayashi S, Neo M, Suzuki J, Kokubo T, Nakamura T. Mechanical properties and osteoconductivity of porous bioactive titanium. Biomaterials 2005;26:6014–23.
[27] Takemoto M, Fujibayashi S, Neo M, Suzuki J, Matsushita T, Kokubo T, et al. Osteoinductive porous titanium implants: effect of sodium removal by dilute HCl treatment. Biomaterials 2006;27:2682–91.
[28] Takemoto M et al. A porous bioactive titanium implant for spinal interbody fusion: an experimental study using a canine model. J Neurosur Spine 2007;7:435–43.
[29] Kokubo T, Takadama H. How useful is SBF in predicting in vivo bone bioactivity? Biomaterials 2006;27:2907–15.

[30] Fujibayashi S, Nakamura T, Nishiguchi S, Tamura J, Uchida M, Kim HM, et al. Bioactive titanium: effect of sodium removal on the bone-bonding ability of bioactive titanium prepared by alkali and heat treatment. J Biomed Mater Res 2001;56:562–70.
[31] Fujibayashi S, Neo M, Kim HM, Kokubo T, Nakamura T. A comparative study between in vivo bone ingrowth and in vitro apatite formation on Na_2O–CaO–SiO_2 glasses. Biomaterials 2003;24:1349–56.
[32] Maniatopoulos C, Rodriguez A, Deporter DA, Melcher AH. An improved method for preparing histological sections of metallic implants. Int J Oral Maxillofac Implants 1986;1:31–7.
[33] Nakamura T, Takemoto M. Osteoconduction and its evaluation. In: Kokubo T, editor. Bioceramics and their clinical applications. Cambridge: Woodhead Publishing; 2008. p. 183–98.
[34] Yang YZ, Tian JM, Tian JT, Chen ZQ, Deng XJ, Zhang DH. Preparation of graded porous titanium coatings on titanium implant materials by plasma spraying. J Biomed Mater Res 2000;52:333–7.
[35] Pattanayak DK et al. Fabrication of bioactive porous Ti metal with structure similar to human cancellous bone by selective laser melting. Bioceramics 2009;22:163–6.
[36] Tanaka K, Takemoto M, Fujibayashi S, Kawanabe K, Matsushita T, Kokubo T, et al. Long-term study of osteoconductivity of bioactive porous titanium metals: effect of sodium removal by dilute HCl treatment. Key Eng Mater 2009;396–398:353–6.

Interface focus

J. R. Soc. Interface (2010) **7**, S503–S513
doi:10.1098/rsif.2010.0129.focus
Published online 5 May 2010

Positively charged bioactive Ti metal prepared by simple chemical and heat treatments

Tadashi Kokubo[1,*], Deepak K. Pattanayak[1], Seiji Yamaguchi[1], Hiroaki Takadama[1], Tomiharu Matsushita[1], Toshiyuki Kawai[2], Mitsuru Takemoto[2], Shunsuke Fujibayashi[2] and Takashi Nakamura[2]

[1]*Department of Biomedical Sciences, Chubu University, Kasugai 487-8501, Japan*
[2]*Department of Orthopedic Surgery, Graduate School of Medicine, Kyoto University, Kyoto 606-8507, Japan*

A highly bioactive bone-bonding Ti metal was obtained when Ti metal was simply heat-treated after a common acid treatment. This bone-bonding property was ascribed to the formation of apatite on the Ti metal in a body environment. The formation of apatite on the Ti metal was induced neither by its surface roughness nor by the rutile phase precipitated on its surface, but by its positively charged surface. The surface of the Ti metal was positively charged because acid groups were adsorbed on titanium hydride formed on the Ti metal by the acid treatment, and remained even after the titanium hydride was transformed into titanium oxide by the subsequent heat treatment. These results provide a new principle based on a positively charged surface for obtaining bioactive materials.

Keywords: bioactive Ti metal; apatite formation; surface charge; chemical treatment; dental implant; orthopaedic implant

1. INTRODUCTION

In general, synthetic materials implanted into bone defects become encapsulated by a fibrous tissue to isolate them from the surrounding bone. Only a few types of ceramic, based on calcium phosphate, have been shown to bond to living bone without the intervention of fibrous tissue at the interface (Kokubo 2008). These are called bioactive ceramics and they are already used clinically as important bone substitutes. However, they are brittle and have poor fracture toughness, and, hence, cannot be used under load-bearing conditions.

In the orthopaedic and dental fields, metallic materials, such as Ti metal and its alloys, are widely used as various implants because of their high fracture toughness and good biocompatibility. However, they do not bond to living bone. As-polished or as-abraded Ti metal is encapsulated by fibrous tissue that isolates it from the surrounding bone when it is implanted into a bone defect (Yan *et al.* 1997; Hacking *et al.* 2002). When a rough texture is produced on its surface by grit blasting or acid etching, Ti can form a direct contact with living bone (Hacking *et al.* 2002). Therefore, some orthopaedic and dental implants have been subjected to grit blasting and/or acid etching (Coelho *et al.* 2009). However, this direct contact itself does not bond the implant to bone. To enable Ti metal and its alloys to bond to bone, hydroxyapatite has been coated on their surfaces using various methods (Leeuwenburgh *et al.* 2008). However, the hydroxyapatite coating is not stable in the living body for long periods.

Early on, we found that a titania gel prepared using a sol–gel method forms a bone-like apatite layer on its surface in an acellular simulated body fluid (SBF) with ion concentrations nearly equal to those of human blood plasma (Li *et al.* 1994). On the other hand, it has been shown for various bioactive ceramics that a material able to form bone-like apatite on its surface in an SBF generally forms the apatite on its surface also in the living body and bonds to living bone through the apatite layer (Kokubo & Takadama 2006). Based on these findings, it was assumed that even Ti metal could form apatite on its surface in the living body and bond to living bone through this apatite layer if it could be modified with a functional group that was effective for the nucleation of apatite on its surface. As expected, it was shown that Ti metal formed with sodium titanate on its surface by an NaOH solution and a subsequent heat treatment induced the formation of apatite on its surface in a living body, so that it can bond to living bone (Kim *et al.* 1996; Yan *et al.* 1997; Nishiguchi *et al.* 2003). This treatment was applied to a porous Ti metal layer of a total artificial hip joint,

*Author for correspondence (kokubo@isc.chubu.ac.jp).

One contribution to a Theme Supplement 'Scaling the heights—challenges in medical materials: an issue in honour of William Bonfield, Part II. Bone and tissue engineering'.

Received 4 March 2010
Accepted 14 April 2010

and the obtained bioactive joint has been used successfully clinically in Japan since 2007 (Kawanabe *et al.* 2009).

However, the apatite-forming ability of the NaOH- and heat-treated Ti metal is liable to decrease when it is stored in a humid environment for long periods, since the sodium ions of the sodium titanate are slowly released via exchange with the H_3O^+ ions in the moisture in the atmosphere. In this study, we show that a highly bioactive Ti metal formed with titanium oxide on its surface, which is stable in a humid environment, is obtained using only a simple heat treatment after a common acid treatment, and that a new principle for obtaining bioactive materials can be proposed based on the mechanism of apatite formation on the bioactive Ti metal.

Several papers have been published on the formation of apatite on the titanium oxide formed on Ti metal after a chemical treatment. Uchida *et al.* (2002) first reported that Ti metal which formed anatase and rutile on its surface by an NaOH solution, water and a heat treatment induced the formation of apatite on its surface in an SBF. Wang *et al.* (2002) reported that Ti metal which formed anatase on its surface by an H_2O_2/HCl solution and a heat treatment induced the formation of apatite on its surface in an SBF. Wu *et al.* (2004) reported that Ti metal which formed anatase and rutile on its surface by HF/HNO_3 and subsequent H_2O_2/$TaCl_2$ solution treatments induced the formation of apatite on its surface in an SBF. Yang *et al.* (2004) reported that Ti metal which formed anatase and rutile on its surface by anodic oxidation using a spark discharge in an H_2SO_4 solution induced the formation of apatite on its surface in an SBF. Lu *et al.* (2007) reported that Ti metal that was treated with strong nitric acid for a long period induced the formation of apatite on its surface in an SBF, although no titanium oxide was detected on its surface. Lu *et al.* (2008) reported that acid-etched Ti metal which formed rutile on its surface by a heat treatment induced the formation of apatite on its surface in an SBF. Pattanayak *et al.* (2009) reported that the apatite-forming ability of Ti metal with rutile and anatase on its surface after soaking in NaOH and HCl solutions, and then a heat treatment, increased with increasing concentration of the HCl solution. However, there is no consensus on the principles governing the apatite-forming ability of titanium oxide on Ti metal.

2. MATERIAL AND METHODS

2.1. Preparation of the Ti metal samples

Commercial pure Ti metal (Kobe Steel, Japan, grade 2, O_2 content = 0.15 wt%) was cut into rectangular samples (dimensions = 10 × 10 × 1 mm^3), and abraded with a no. 400 diamond abrasive plate. All the abraded samples were washed with acetone, 2-propanol and ultrapure water for a period of 30 min each in an ultrasonic cleaner, and then dried overnight in an oven at 40°C.

The samples were soaked in 20 ml of a mixture of 66.3 per cent H_2SO_4 (w/w) solution (Kanto Chemical Co., Inc., Japan) and 10.6 per cent HCl (w/w) solution (Kanto Chemical Co., Inc.) in a weight ratio of 1 : 1 at 70°C for a period of 1 h in an oil bath shaken at 120 strokes min^{-1}, then gently washed with ultrapure water and dried overnight in an oven at 40°C. This mixed acid solution is the same etchant used for one of the commercial dental implants (Takeuchi *et al.* 2005).

The acid-treated samples were heated to temperatures in the range 400–800°C at a rate of 5°C min^{-1} in an Fe–Cr furnace in air. The samples were kept at the desired temperature for a period of 1 h, and then allowed to cool to room temperature at the natural rate of the furnace. As a reference, the abraded samples were heat-treated using the same method without being subjected to an acid treatment.

2.2. Examination of the apatite-forming ability of Ti metal in an SBF

The samples subjected to the acid and heat treatments, and those subjected to only the heat treatment, were soaked in 30 ml of an acellular SBF with ion concentrations nearly equal to those of human blood plasma at 36.5°C (Na^+ = 142.0, K^+ = 5.0, Mg^{2+} = 1.5, Ca^{2+} = 2.5, Cl^- = 147.8, HCO_3^- = 4.2, HPO_4^{2-} = 1.0 and SO_4^{2-} = 0.5 mM; Kokubo & Takadama 2006). The SBF was prepared by dissolving reagent grade NaCl, $NaHCO_3$, KCl, $K_2HPO_4 \cdot 3H_2O$, $MgCl_2 \cdot 6H_2O$, $CaCl_2$ and Na_2SO_4 (Nacalai Tesque Inc., Japan) into ultrapure water, and then buffering the solution at pH = 7.4 using tris-hydroxymethylaminomethane ($(CH_2OH)_3CNH_2$) and 1 M HCl (Nacalai Tesque Inc.). The samples were removed from the SBF after 1 day, gently washed with ultrapure water and dried in an oven at 40°C. The formation of apatite on the sample surface was examined using scanning electron microscopy (SEM) and thin film X-ray diffraction (TF-XRD) employing the methods described in the next section.

To examine the stability of the apatite-forming ability in a humid environment, the acid- and heat-treated samples were kept under an atmosphere of 95 per cent relative humidity at 80°C for a period of one week, and the formation of apatite on the surface in an SBF was examined using SEM and TF-XRD.

2.3. Analysis of the surface of the Ti metal samples

2.3.1. Scanning electron microscopy. The surface and cross-sectional area of the Ti metal samples subjected to both the acid and heat treatments, to the heat treatment alone, and those subsequently soaked in an SBF were coated with a Pt/Pd film and observed under a field-emission scanning electron microscope (FE-SEM; S-4300, Hitachi Co., Japan), using an acceleration voltage of 15 kV.

2.3.2. Thin film X-ray diffraction. The surface of the Ti metal samples subjected to both the acid and heat treatments, to the heat treatment alone, and those subsequently soaked in an SBF were analysed using TF-XRD (model RNT-2500, Rigaku Co., Japan),

employing a CuKα X-ray source operating at 50 kV and 200 mA. The glancing angle of the incident beam was set to an angle of 1° against the sample surface.

2.3.3. Surface roughness measurements. The surface roughness of the Ti metal samples subjected to the acid and heat treatments was measured using a surface roughness testing system (Surftest model SV-2000, Mitutoyo Co., Japan) using a stylus with a diameter of 2 μm. Based on the data in the JIS standard 1994, the measuring length, evaluation length and cut-off wavelength used were 2.5, 12.5 and 2.5 mm, respectively. Seven measurements were performed for each sample and averaged.

2.3.4. Scratch resistance measurements. The scratch resistance of the surface layer formed on the Ti metal samples by the acid and heat treatments or the heat treatment alone was measured using a thin film scratch tester (model CSR-2000, Rhesca Co., Japan) employing a stylus with a diameter of 5 μm with a spring constant of 200 g mm^{-1}. Based on the data in the JIS R-3255 standard, the amplitude, scratch speed and loading rate used were 100 μm, 10 μm s^{-1} and 100 mN min^{-1}, respectively. Eight to 10 measurements were carried out for each sample, and the average value was used in our analysis.

2.3.5. Zeta potential measurements. Titanium metal plates (size = 13 × 33 × 1 mm^3) were prepared using the same method described in §2.1, and these were subjected to the acid and heat treatments, or to the heat treatment alone, at various temperatures. The volume of the acid solution was increased to 30 ml in the acid treatment, because the surface area of the sample was larger than that used for the other surface analysis measurements. Thus, the treated Ti metal samples were grounded to allow for leakage of any stray charge, and they were immediately set in a zeta potential and particle size analyser (model ELS-Z1, Otsuka Electronics Co., Japan) using a glass cell for the plate sample. The zeta potentials of the samples were measured under an applied voltage of 40 V in a 10 mM NaCl solution. The dispersant monitoring particles of polystyrene latex (size = 500 nm) were coated with hydroxyl propyl cellulose. Five samples were measured for each experimental condition and the average reported in our analysis.

2.3.6. X-ray photoelectron spectroscopy. The surfaces of the Ti metal samples soaked in an SBF for various periods after the acid and heat treatments, or the heat treatment alone, were analysed using X-ray photoelectron spectroscopy (XPS, ESCA-3300KM, Shimadzu Co., Japan) as a function of the soaking time in the SBF. In our analysis, MgKα radiation ($\lambda = 9.8903$ Å) was used as the X-ray source. The XPS take-off angle was set at 45°, which enabled the system to detect photoelectrons to a depth of 5–10 nm from the surface. The binding energies of the measured spectra were calibrated with reference to the C_{1s} peak of the surfactant CH_2 groups on the substrate at 284.6 eV.

2.3.7. Radio frequency (RF) glow discharge optical emission spectroscopy. The depth profiles of various elements on the surface of the Ti metal samples subjected to the acid and heat treatments were analysed using RF glow discharge optical emission spectroscopy (GD-OES, GD-Profiler 2, Horiba Co., Japan) under Ar sputtering at an Ar pressure of 600 Pa. A RF electric field with a power of 35 W was applied at a regular interval of 20 ms.

2.4. Examination of the bone-bonding ability of Ti metal

The Animal Research Committee of the Graduate School of Medicine, Kyoto University, Japan, approved our animal studies. Rectangular samples (size = 15 × 10 × 2 mm^3) of Ti metal subjected to the acid and heat treatments, or the heat treatment alone, were sterilized with ethylene oxide gas and implanted into metaphyses of the tibiae of mature male Japanese white rabbits weighing 2.8–3.2 kg. The surgical methods used have been described previously (Nakamura *et al.* 1985). After four weeks' implantation, the rabbits were sacrificed using an overdose of intravenous pentobarbital sodium. The segments of the proximal tibiae metaphyses containing the implanted samples were retrieved. The bone tissue surrounding the implants was removed on both sides and at the ends using a dental burr. Traction was applied vertically to the sample surface at a crosshead speed of 35 mm min^{-1} using an Instron-type autograph (model 1011, Aikon Engineering Co., Japan). The detaching failure load was recorded when the sample was detached from the bone. Five measurements were performed for each experimental condition and the average value recorded.

Other segments of the tibiae containing the implanted samples were fixed in 10 per cent phosphate-buffered formalin, dehydrated using ethanol, and embedded in polyester resin. Sections with a thickness of 500 μm were cut, bound to a transparent acrylic plate, and ground to a thickness of 40–50 μm. These samples were stained using Stevenel's blue and Van Gieson's picro-fuchsin. A histological evaluation was performed on each stained section using transmitted light microscopy (model Eclipse 80i, Nikon Co., Japan).

3. RESULTS

3.1. Change in the surface structure of the Ti metal after the acid and heat treatments

Figure 1 shows FE-SEM photographs of the surfaces of Ti metal samples as-abraded, and after being heat-treated at 600°C and 800°C. The abraded sample had a smooth surface, but its surface roughness increased a little with increasing temperature of the heat treatment.

Figure 2 shows FE-SEM photographs of the surfaces of Ti metal samples that had been subjected to the acid

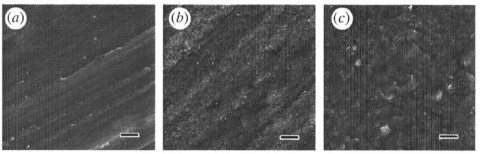

Figure 1. FE-SEM photographs of surfaces of Ti metals as-abraded, and subsequently heat-treated at different temperatures. (*a*) Before heat treatment, (*b*) heat-treated at 600°C and (*c*) heat-treated at 800°C. Scale bars, 1 μm.

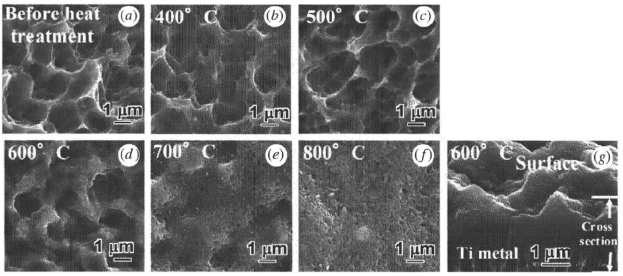

Figure 2. FE-SEM photographs of surfaces and a cross section of Ti metals as acid-treated, and subsequently heat-treated, at various temperatures. (*a*) Before heat treatment and heat-treated at (*b*) 400°C, (*c*) 500°C, (*d*) 600°C, (*e*) 700°C, (*f*) 800°C and (*g*) a cross section of Ti metal at 600°C.

treatment and subsequently heat-treated at various temperatures up to 800°C. A cross-sectional view of a sample heat-treated at 600°C is also shown in figure 2. A surface roughness was produced on the Ti metal sample by the acid treatment, and this remained unchanged up to 600°C, but the sample surface roughness decreased above 700°C.

According to our surface roughness measurements, the values of R_a and R_z were $R_a = 0.99 \pm 0.07$ and $R_z = 8.87 \pm 0.94$ μm for the samples that had been acid-treated, and $R_a = 0.99 \pm 0.17$ and $R_z = 7.33 \pm 0.83$ μm for the samples that had been heat-treated at 600°C.

The scratch resistance of the Ti metal samples as-abraded and acid-treated were very low, about 1–2 mN. Both of these samples showed a marked increase up to 40–55 mN after the subsequent heat treatments at 600–800°C.

Figure 3*a*,*b* shows thin film X-ray diffraction patterns of the surfaces of the Ti metal samples subjected to heat treatment at various temperatures, without and after the acid treatment, respectively. The as-abraded sample consisted of α titanium, whereas the acid-treated sample formed a titanium hydride layer (TiHx, where $0 < x < 2$) on its surface. Despite these differences, both of these samples began to precipitate rutile around 500°C on their surfaces, and the rutile content increased with increasing heat-treatment temperature up to 800°C. It is apparent from these results that the increase in surface roughness of the abraded sample, the decrease in surface roughness of the acid-treated sample, and the increase in the scratch resistance of the abraded and acid-treated samples with increasing temperature of the heat treatment are all attributed to the precipitation of the rutile on the surface of the Ti metals.

3.2. *Change in the apatite-forming ability of Ti metal in an SBF after acid and heat treatments*

Figure 4 shows FE-SEM photographs of the surface of Ti metal samples soaked in an SBF for a period of 1 day, after being abraded and subsequently heat-treated at 600 and 800°C. No deposit was observed on these surfaces.

Figure 5 shows FE-SEM photographs of the surfaces of Ti metal samples soaked in an SBF for a period of 1 day, after being treated with acid and subsequently heat-treated at various temperatures up to 800°C. The cross section of a sample soaked in an SBF for a period of 1 day after the acid and heat treatments at 600°C is also shown in figure 5.

Figure 6 shows TF-XRD patterns of the surfaces of Ti metal samples soaked in an SBF for a period of 1 day, after being treated with acid and subsequently heat-treated at various temperatures. The round particles observed on the surfaces of the Ti metal samples in figure 5 are identified as being apatite from TF-XRD patterns of figure 6, although its detailed structure is not clear from these TF-XRD patterns (Lu & Leng 2004). From figure 5, it can be seen that apatite was deposited actively only on the surface of Ti metal

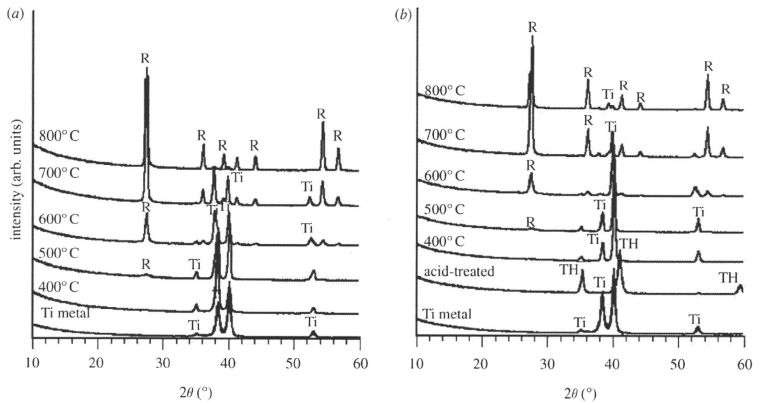

Figure 3. TF-XRD patterns of surfaces of Ti metals heat-treated at various temperatures (*a*) without and (*b*) after acid treatment. R, rutile; Ti, α titanium; TH, TiH*x*.

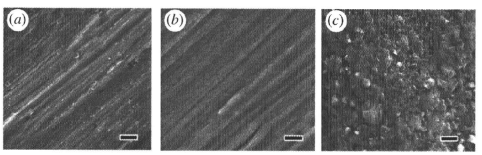

Figure 4. FE-SEM photographs of surfaces of the Ti metals soaked in SBF for 1 day, after being abraded, and subsequently heat-treated at different temperatures. (*a*) Before heat treatment, (*b*) heat-treated at 600°C and (*c*) heat-treated at 800°C. Scale bars, 2 μm.

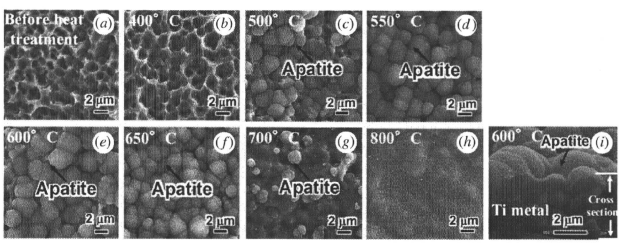

Figure 5. FE-SEM photographs of surfaces and a cross section of Ti metals soaked in SBF for 1 day, after being heat-treated at various temperatures following the acid treatment. (*a*) Before heat treatment and heat-treated at (*b*) 400°C, (*c*) 500°C, (*d*) 550°C, (*e*) 600°C, (*f*) 650°C, (*g*) 700°C, (*h*) 800°C and (*i*) a cross section of Ti metal at 600°C.

samples that had been heat-treated at temperatures from 500 to 650°C after an acid treatment.

Figure 7 shows an FE-SEM photograph of the surface of a Ti metal sample soaked in an SBF for a period of 1 day that had been kept under an atmosphere of 95 per cent relative humidity at 80°C for a period of one week following an acid and heat treatment at 600°C. The apatite-forming ability of the acid- and heat-treated Ti metal sample was only a little decreased even after it was kept in a humid environment for a period of one week.

3.3. Change in the zeta potential of Ti metal after acid and heat treatments

Figure 8 shows the zeta potentials of the surfaces of Ti metal samples heat-treated at various temperatures without and after an acid treatment. The zeta

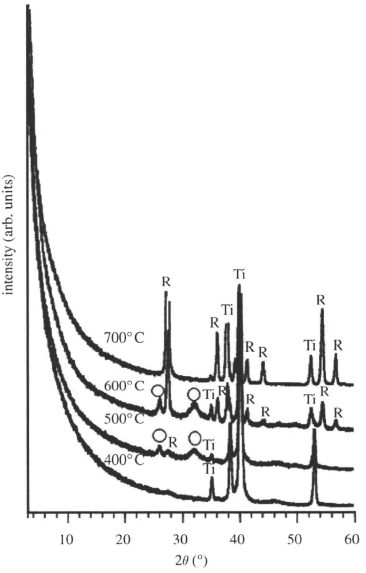

Figure 6. TF-XRD patterns of the surfaces of Ti metals soaked in SBF for 1 day after being heat-treated at various temperatures following acid treatment. Ti, α titanium; R, rutile; open circle, apatite.

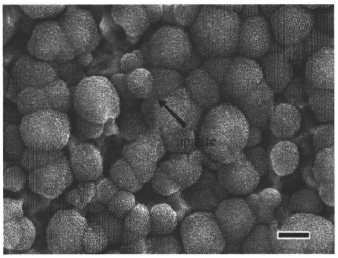

Figure 7. FE-SEM photograph of the surface of Ti metal soaked in SBF for 1 day, after being kept in a humid environment for one week following the acid and heat treatments at 600°C (scale bar, 2 μm).

potentials of the samples that had been heat-treated at temperatures lower than 500°C were not able to be measured, since there was no or only a thin insulating titanium oxide layer formed on their surface (see figure 3). The Ti metal samples treated without being subjected to the acid treatment showed low zeta potentials, around zero, irrespective of the temperature of the heat treatment, whereas those heat-treated after

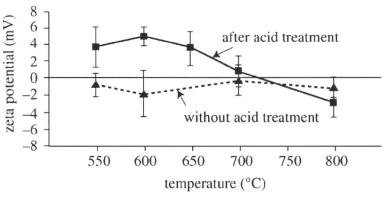

Figure 8. Zeta potentials of surfaces of Ti metals heat-treated at various temperatures without and after acid treatment.

the acid treatment showed positive zeta potentials when heat-treated at temperatures in the range 550–650°C.

3.4. Change in the XPS spectra of Ti metal after acid and heat treatments

Figure 9 shows the XPS spectra of the surfaces of the Ti metal samples as-abraded and subsequently heat-treated at 600°C as a function of the soaking time in the SBF. The as-abraded sample adsorbed only a small amount of the calcium and phosphate ions, almost simultaneously, on its surface, even after 12 h in the SBF, and this property was unchanged after heat treatment at 600°C.

Figure 10 shows the XPS spectra of the surfaces of the Ti metal samples that had been treated with acid and subsequently heat-treated at 600°C as a function of the soaking time in the SBF. The acid-treated sample also adsorbed only a small amount of the calcium and phosphate ions, almost simultaneously, in the SBF, whereas the sample heat-treated at 600°C after the acid treatment initially adsorbed a large amount of phosphate ions preferentially on its surface, and then later adsorbed a large amount of calcium ions.

3.5. Change in the GD-OES spectra of Ti metal after acid and heat treatments

Figure 11 shows the depth profile of the GD-OES spectra of Ti metal samples that were treated with acid, subsequently heat-treated at 600°C, and then kept under an atmosphere of 95 per cent relative humidity at 80°C for a period of one week. Large amounts of H and O, besides Ti atoms, were detected in the surface layer of the samples that were treated with acid and subsequently heat-treated, respectively, because of the presence of titanium hydride and titanium oxide on their surfaces. Besides the presence of H, O and Ti, a large amount of Cl and S atoms was detected in the surface layer of the samples that had been treated with acid, and a considerable amount of these atoms was detected even after the subsequent heat treatment at 600°C and being kept in a humid environment for a period of one week.

3.6. Bonding of Ti metal to bone

The as-abraded titanium metal samples and those subsequently heat-treated at 600°C showed a detaching failure load of 1.86 ± 1.72 and 6.12 ± 3.43 N,

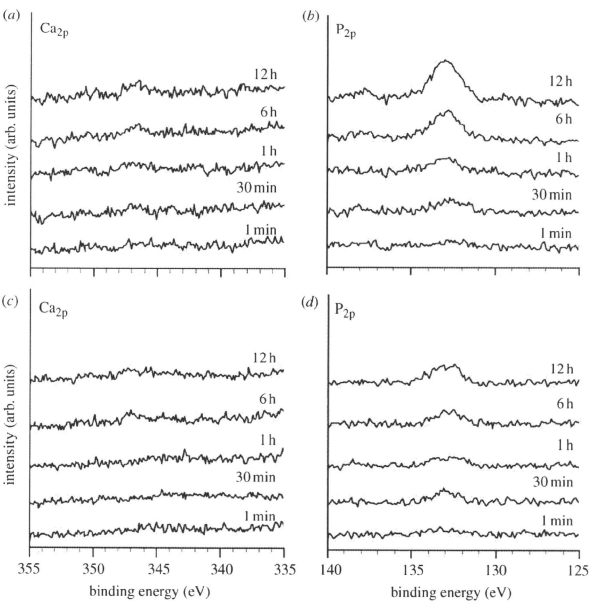

Figure 9. (*a*,*b*) XPS spectra of the surfaces of Ti metals abraded and (*c*,*d*) subsequently heat-treated at 600°C, as a function of soaking time in SBF.

respectively, when they were implanted into the tibia of a rabbit and subjected to the detaching test at four weeks after implantation. The acid-treated samples and those subsequently heat-treated at 600°C showed a failure load of 4.91 ± 1.94 and 13.3 ± 4.67 N, respectively. The failure load of the abraded sample was only slightly increased by the heat treatment or acid treatment. However, it was increased markedly by a heat treatment after the acid treatment.

Figure 12 shows the light micrographs of an interface with the living bone of a sample that was heat-treated at 600°C after the acid treatment. Bone had grown along the surface of the Ti metal sample and it was in direct contact with the sample without the intervention of any fibrous tissue.

4. DISCUSSION

It is apparent from the experimental results described above that a high apatite-forming ability in an SBF is conferred on Ti metal by neither a heat treatment alone nor an acid treatment alone, but is conferred by a heat treatment after an acid treatment. Titanium metal subjected to a heat treatment after an acid treatment to confer a high apatite-forming ability was confirmed to be directly in contact with newly grown bone and formed tight bonding to the bone in the animal experiments. This means that bioactive Ti metal can be obtained by a simple heat treatment after a common acid treatment. The high apatite-forming ability of our prepared Ti metal was confirmed to be maintained, even when kept in a humid environment for a long period. It was also shown that our prepared Ti metal showed a considerably high scratch resistance. Because of these properties, our prepared bioactive Ti metal is believed to be useful for various types of implant in the dental and orthopaedic fields.

It should be noted here that porous bioactive Ti metal with titanium oxide on its surface after NaOH, HCl and heat treatment exhibits high osteoinductivity, which is poor for porous Ti metal with sodium titanate on its surface after NaOH and heat treatment, in addition to the observed osteoconductivity (Takemoto *et al.* 2006). That is, these samples show active bone formation not only in bone defects but also in muscles. The higher osteoinductivity of the former samples compared with the latter is considered to be attributed to the lack of ions, which, in the latter, are released to form unfavourable conditions for the cells by increasing the pH. In view of this fact, the bioactive Ti metal formed with the titanium oxide on its surface using the present method can also be expected to exhibit a high osteoinductivity. This is now being investigated.

Although detailed results of the animal experiments described in §2.4 will be published elsewhere, the tight

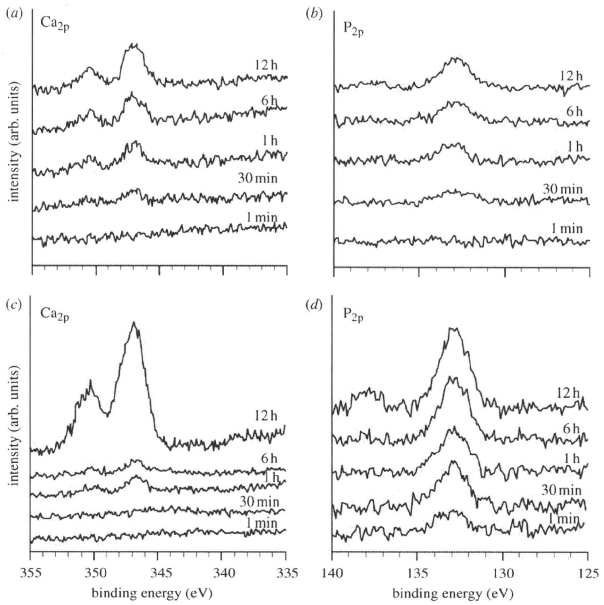

Figure 10. (*a*,*b*) XPS spectra of surfaces of Ti metals acid-treated and (*c*,*d*) subsequently heat-treated at 600°C, as a function of soaking time in SBF.

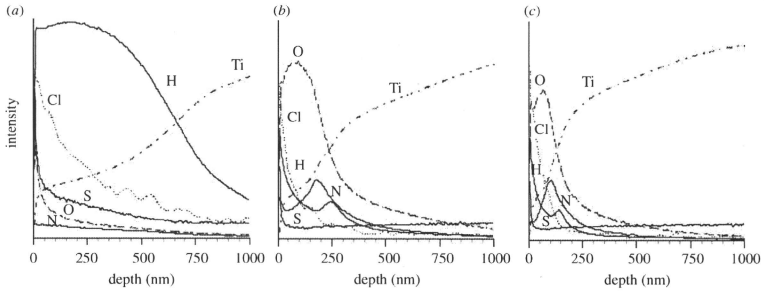

Figure 11. (*a*) Depth profiles of GD-OES spectra of Ti metals acid-treated, (*b*) subsequently heat-treated at 600°C and (*c*) kept in a humid environment.

bonding of the Ti metal heat-treated after the acid treatment can be attributed to the formation of apatite on its surface in the living body. We are concerned as to the reason why Ti metal forms apatite on its surface in a body environment when it is heat-treated at temperatures in the range 500–650°C after an acid treatment. A rough surface was produced on the Ti metal by the acid treatment, but the surface roughness was unchanged in the temperature range 500–650°C from before heat treatment (see figure 2). Therefore, the formation of apatite on our Ti metal samples cannot be attributed to their surface roughness. The acid-treated Ti metal samples precipitated rutile on their surface when heat-treated at 500–650°C, but the Ti metal samples without an acid treatment also precipitated the same phase in the same temperature range (see figure 3).

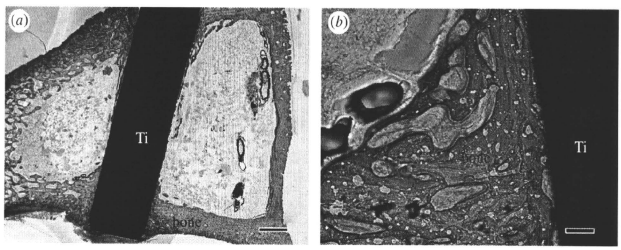

Figure 12. Light micrographs of strained sections of acid- and heat-treated Ti metal implanted into a rabbit tibia for four weeks. Scale bars, (*a*) 1 mm, (*b*) 100 μm.

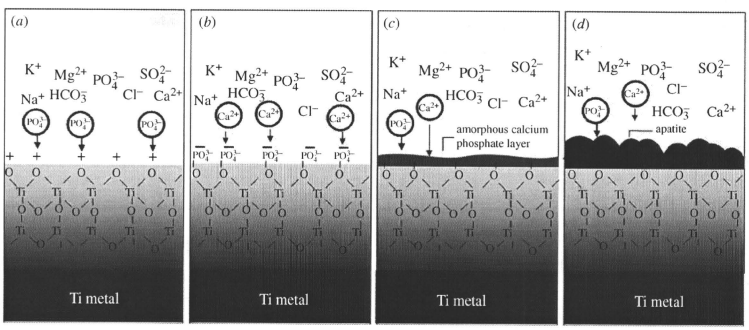

Figure 13. Process of formation of apatite on positively charged Ti metal in SBF. Apatite is formed by the process shown in (*a*–*d*).

Therefore, the formation of apatite on our Ti metal samples cannot be attributed to a specific crystalline phase.

The most probable reason for the formation of apatite on our Ti metal samples is their positive surface charge. Figure 8 shows that only the Ti metal samples that were heat-treated at temperatures of 550–650°C after an acid treatment showed a positive zeta potential. Although the zeta potential of Ti metal heat-treated at 500°C after an acid treatment was not measured, it is assumed to have a positive value, since the Ti metal sample heat-treated at 500°C had a titanium oxide layer on its surface, similar to Ti metal samples heat-treated at 550–650°C, even though this layer was very thin (see figure 3). The zeta potentials of the Ti metal samples acid-treated and subsequently heat-treated at temperatures below 400°C also could not be measured, because the insulating titanium oxide layer was not formed on their surfaces (see figure 3). This means that their surfaces are electrically conductive, and hence their zeta potentials are zero.

Our question now is to find the reason why the positively charged titanium oxide on Ti metal forms apatite on its surface in the body environment. The XPS spectra of Ti metal shown in figure 10 show that Ti metal heat-treated at 600°C after an acid treatment preferentially adsorbs a large amount of phosphate ions first, and then later it also adsorbs calcium ions. This result indicates that positively charged titanium oxide induces the formation of apatite on its surface by the process shown in figure 13. The positively charged titanium oxide first selectively adsorbs the negatively charged phosphate ions on its surface. As the phosphate ions begin to accumulate, the surface becomes negatively charged, and, hence, combines with the positively charged calcium ions to form calcium phosphate. The calcium phosphate formed eventually transforms into stable crystalline apatite.

This process of the formation of apatite on a positively charged titanium oxide layer contrasts with that where sodium titanate is formed on Ti metal after NaOH and heat treatments (Kim *et al.* 2003). In this case, the sodium titanate releases Na^+ ions via exchange with the H_3O^+ ions in the body fluid to form Ti–OH groups on its surface. The Ti–OH groups formed are negatively charged (Kokubo *et al.* 1982), since the pH of the surrounding body fluid is increased by the Na^+ ions released, and, hence, combines with the positively charged Ca^{2+} ions in the body fluid to form calcium titanate. As the Ca^{2+} ions

accumulate, the surface becomes positively charged and combines with the negatively charged phosphate ions to form calcium phosphate. Thus, the calcium phosphate formed eventually transforms into stable crystalline apatite. Ever since discovering this apatite-forming process, it was believed that a negatively charged surface is essential for obtaining bioactive materials. However, the present results show that a positively charged surface can also provide bioactive materials by inducing the formation of apatite. This finding provides a new principle for the development of bioactive materials. Generally, Ti metal exhibits surface charge around zero in a body environment independent of heat treatment, as shown for a Ti metal sample without acid treatment in figure 8, and, hence, does not induce apatite formation (see figure 4). However, the present results indicate that Ti metal is negatively charged on its surface in a body environment if it has been subjected to alkali and heat treatments, and it is positively charged on its surface if it has been subjected to acid and heat treatments, and, hence, it can induce apatite formation on its surface in a body environment to give bone-bonding ability.

The reason why Ti metal heat-treated at 500–650°C after an acid treatment is positively charged is interpreted in terms of figure 11. Acid groups, such as chloride and sulphate ions, were adsorbed onto the surface of, and incorporated into, the titanium hydride layer on the surface of the Ti metal formed during the acid treatment, and a considerable amount of these ions remained in the surface layer, even after the titanium hydride was transformed into titanium oxide by the heat treatment at 600°C. These acid groups could be released from the surface to form an acidic environment in the vicinity of the surface when the Ti metal is soaked in an SBF. As a result, the surface would be positively charged, since titanium oxide is positively charged in an acidic environment (Kokubo *et al.* 1982; Gold *et al.* 1989; Textor *et al.* 2001). The Ti metal samples heat-treated at temperatures lower than 400°C after an acid treatment had no insulating oxide layer on their surface, and, hence, their surface was not charged and so did not induce formation of apatite in an SBF. The Ti metal samples heat-treated at temperatures higher than 700°C after the acid treatment decomposed incorporated ions on heat treatment, and, hence, their surface was not positively charged, and so did not induce the formation of apatite. Figure 11 shows that the incorporated ions almost remain on the surface of the Ti metal heat-treated at 600°C after the acid treatment, even after the Ti metal was kept in a humid environment for a period of one week. As a result, the apatite-forming ability of this Ti metal was only a little decreased, even after it was kept in a humid environment.

These results indicate that the requirement for obtaining a positively charged Ti metal that is effective for inducing the formation of apatite on its surface in a body environment is the formation of an electrically insulating oxide layer on its surface, and the adsorption of acid groups on its surface. These requirements are met only by the common acid treatment and subsequent heat treatment at moderately high temperatures. This indicates that the apatite formation of the Ti metal heat-treated after acid treatment does not depend upon the kind of acid solutions, but upon the pH of the solutions. This has already been confirmed experimentally and will be published elsewhere.

In view of this fact, most of the chemical and heat treatments for obtaining bioactive Ti metal by forming a titanium oxide on its surface, which were cited in §1, can be interpreted in terms of the method that forms a layer that can meet these requirements on the surface of the Ti metal.

Zhao *et al.* (2005, 2008) reported that a plasma-sprayed TiO_2 coated layer with a rutile phase showed a high apatite-forming ability in an SBF when treated with an acid solution, such as H_2SO_4 and HNO_3. Kokubo *et al.* (2008) reported that a titania gel layer coated on polyethylene terephthalate using a sol–gel method formed apatite on its surface in an SBF when it was treated with an HCl solution at 80°C for a period of 8 days. These results can also be interpreted in terms of the formation of a titanium oxide layer containing adsorbed acid groups on its surface to give a positive surface charge in an SBF.

5. SUMMARY

- An ability to form apatite in an SBF was conferred on Ti metal neither by an H_2SO_4/HCl mixed acid treatment alone nor by a heat treatment alone, but by a heat treatment at 500–650°C after the acid treatment. The apatite-forming ability was hardly decreased, even after the Ti metal was maintained in a humid environment for a long period. The acid- and heat-treated Ti metal showed a high scratch resistance. These are important properties for clinical applications of Ti metal.
- Ti metal that was heat-treated at 600°C after the acid treatment was confirmed to be in direct contact with living bone and tightly bonded to it. This tight bonding was attributed to the formation of apatite on the surface of the Ti metal in a body environment.
- The formation of apatite on Ti metal that had been heat-treated at 500–650°C after an acid treatment was attributed neither to the roughness of the surface nor to the rutile phase that had precipitated on the surface, but to the positive charge on the surface.
- The positive charge on the Ti metal was shown to be formed by the adsorption of acid groups on the surfaces by the acid treatment, and by the formation of a non-conducting titanium oxide layer on the surface by the subsequent heat treatment.
- A new principle for obtaining bioactive materials based on a positively charged surface has been proposed.

This work was supported in part by a Grant-in-Aid from the Ministry of Health, Labour, and Welfare of Japan (H21-*Trans*-Ippan-003) and by a Grant-in-Aid for Scientific Research (A) from the Ministry of Education, Culture, Sports, Science and Technology of Japan (19200039).

REFERENCES

Coelho, P. G., Granjeiro, J. M., Romanos, G. E., Suzuki, M., Silva, N. R. F., Cardaropoli, G., Thompson, V. P. & Lemons, J. E. 2009 Basic research methods and current trends of dental implant surfaces. *J. Biomed. Mater. Res.* **88B**, 579–596. (doi:10.1002/jbm.b.31264)

Gold, J. M., Schmidt, M. & Steinemann, S. G. 1989 XPS study of amino-acid adsorption to titanium surface. *Helv. Phys. Acta* **62**, 246–249.

Hacking, S. A., Tanzer, M., Harvey, E. J., Krygier, J. J. & Bobyn, J. D. 2002 Relative contributions of chemistry and topography to the osseointegration of hydroxyapatite coatings. *Clin. Orthopaed. Relat. Res.* **405**, 24–38. (doi:10.1097/00003086-200212000-00004)

Kawanabe, K., Ise, K., Goto, K., Akiyama, H., Nakamura, T., Kaneuji, A., Sugimori, T. & Matsumoto, T. 2009 A new cementless total hip arthoplasty with bioactive titanium porous-coating by alkaline and heat treatment: average 4.8-year results. *J. Biomed. Mater. Res.* **90B**, 476–481. (doi:10.1002/jbm.b.31309)

Kim, H. M., Miyaji, F., Kokubo, T. & Nakamura, T. 1996 Preparation of bioactive Ti and its alloy via simple chemical surface treatment. *J. Biomed. Mater. Res.* **32**, 409–417. (doi:10.1002/(SICI)1097-4636(199611)32:3<409::AID-JBM14>3.0.CO;2-B)

Kim, H. M., Himeno, T., Kawashita, M., Lee, J. H., Kokubo, T. & Nakamura, T. 2003 Surface potential change in bioactive titanium metal during the process of apatite formation in simulated body fluid. *J. Biomed. Mater. Res.* **67A**, 1305–1309. (doi:10.1002/jbm.a.20039)

Kokubo, T. 2008 *Bioceramics and their clinical applications.* Cambridge, UK: Woodhead Publishing.

Kokubo, T. & Takadama, H. 2006 How useful is SBF in predicting *in vivo* bone bioactivity? *Biomaterials* **27**, 2907–2915. (doi:10.1016/j.biomaterials.2006.01.017)

Kokubo, T., Takagi, H. & Tashiro, M. 1982 Alkaline durability of $BaO-TiO_2-SiO_2$ glasses. *J. Non-Cryst. Solids* **52**, 427–433. (doi:10.1016/0022-3093(82)90317-9)

Kokubo, T., Ueda, T., Kawashita, M., Ikuhara, Y., Takaoka, G. H. & Nakamura, T. 2008 PET fiber fabrics modified with bioactive titanium oxide for bone substitutes. *J. Mater. Sci.* **19**, 695–702. (doi:10.1007/s10856-007-3103-9)

Leeuwenburgh, S. C. G., Wolke, J. G. C., Jansen, J. A. & de Groot, K. 2008 Calcium phosphate coatings. In *Bioceramics and their clinical applications* (ed. T. Kokubo), pp. 464–484. Cambridge, UK: Woodhead Publishing.

Li, P., Ohtsuki, C., Kokubo, T., Nakanishi, K., Soga, N., Nakamura, T., Yamamuro, T. & de Groot, K. 1994 A role of hydrated silica, titania and alumina in forming biologically active bone-like apatite on implant. *J. Biomed. Mater. Res.* **28**, 7–15. (doi:10.1002/jbm.820280103)

Lu, X. & Leng, Y. 2004 TEM study of calcium phosphate precipitation on bioactive titanium surfaces. *Biomaterials* **25**, 1779–1786. (doi:10.1016/j.biomaterials.2003.08.028)

Lu, X., Zhao, Z. & Leng, Y. 2007 Biomimetic calcium phosphate coatings on nitric acid treated titanium surfaces. *Mater. Sci. Eng. C* **27**, 700–708. (doi:10.1016/j.msec.2006.06.030)

Lu, X., Wang, Y., Yang, X., Zhang, Q., Zhao, Z., Weng, L. T. & Leng, Y. 2008 Spectroscopic analysis of titanium surface functional groups under various surface modification and their behaviors *in vitro* and *in vivo*. *J. Biomed. Mater. Res* **84A**, 523–534. (doi:10.1002/jbm.a.31471)

Nakamura, T., Yamamuro, T. & Higashi, S. 1985 A new glass ceramic for bone replacement: evaluation of its bonding to bone tissue. *J. Biomed. Mater. Res.* **19**, 685–698. (doi:10.1002/jbm.820190608)

Nishiguchi, S., Fujibayashi, S., Kim, H. M., Kokubo, T. & Nakamura, T. 2003 Biology of alkali- and heat-treated titanium implants. *J. Biomed. Mater. Res.* **67A**, 26–35. (doi:10.1002/jbm.a.10540)

Pattanayak, D. K., Kawai, T., Matsushita, T., Takadama, H., Nakamura, T. & Kokubo, T. 2009 Effect of HCl concentrations on apatite-forming ability of NaOH–HCl- and heat-treated titanium metal. *J. Mater. Sci.* **20**, 2401–2411. (doi:10.1007/s10856-009-3815-0)

Takemoto, M., Fujibayashi, S., Neo, M., Suzuki, J., Matsushita, T., Kokubo, T. & Nakamura, T. 2006 Osteoinductive porous titanium implants: effect of sodium removal by dilute HCl treatment. *Biomaterials* **27**, 2682–2691. (doi:10.1016/j.biomaterials.2005.12.014)

Takeuchi, K., Saruwatari, L., Nakamura, H. K., Yang, J. M. & Ogawa, T. 2005 Enhanced intrinsic biomechanical properties of osteoblastic mineralized tissue on roughened titanium surface. *J. Biomed. Mater. Res.* **72A**, 296–305. (doi:10.1002/jbm.a.30227)

Textor, M., Sittig, C., Frauchiger, V., Tosatti, S. & Brunette, D. M. 2001 Properties and biological significance of natural oxide films on titanium and its alloys. In *Titanium in medicine* (eds D. M. Brunette, P. Tengvall, M. Textor & P. Thomsen), pp. 171–230. Berlin, Germany: Springer.

Uchida, M., Kim, H.-M., Kokubo, T., Fujibayashi, S. & Nakamura, T. 2002 Effect of water treatment on the apatite-forming ability of NaOH-treated titanium metal. *J. Biomed. Mater. Res.* **63**, 522–530. (doi:10.1002/jbm.10304)

Wang, X. X., Hayakawa, S., Tsuru, K. & Osaka, A. 2002 Bioactive titania gel layers formed by chemical treatment of Ti substrate with a H_2O_2/HCl solution. *Biomaterials* **23**, 1353–1357. (doi:10.1016/S0142-9612(01)00254-X)

Wu, J. M., Hayakawa, S., Tsuru, K. & Osaka, A. 2004 Low-temperature preparation of anatase and rutile layers on titanium substrates and their ability to induce *in vitro* apatite deposition. *J. Am. Ceram. Soc.* **87**, 1635–1642. (doi:0.1111/j.1551-2916.2004.01635.x)

Yan, W. Q., Nakamura, T., Kobayashi, M., Kim, H. M., Miyaji, F. & Kokubo, T. 1997 Bonding of chemically treated titanium implants to bone. *J. Biomed. Mater. Res.* **37**, 267–275. (doi:0.1002/(SICI)1097-4636(199711)37:2<267::AID-JBM17>3.0.CO;2-B)

Yang, B., Uchida, M., Kim, H. M., Zhang, X. & Kokubo, T. 2004 Preparation of bioactive titanium metal via anodic oxidation treatment. *Biomaterials* **25**, 1003–1010. (doi:10.1016/S0142-9612(03)00626-4)

Zhao, X., Liu, X. & Ding, C. 2005 Acid induced bioactive titania surface. *J. Biomed. Mater. Res.* **75A**, 888–894. (doi:10.1002/jbm.a.30485)

Zhao, X., Liu, X., You, J., Chen, Z. & Ding, C. 2008 Bioactivity and cytocompatibility of plasma-sprayed titania coating treated by sulfuric acid treatment. *Surf. Coat. Technol.* **202**, 3221–3226. (doi:10.1016/j.surfcoat.2007.11.026)

Acta Biomaterialia 6 (2010) 2836–2842

Contents lists available at ScienceDirect

Acta Biomaterialia

journal homepage: www.elsevier.com/locate/actabiomat

Preparation of bioactive Ti metal surface enriched with calcium ions by chemical treatment

Takashi Kizuki [a,*], Hiroaki Takadama [a], Tomiharu Matsushita [a], Takashi Nakamura [b], Tadashi Kokubo [a]

[a] Department of Biomedical Sciences, College of Life and Health Sciences, Chubu University, 1200 Matsumoto-cho, Kasugai, Aichi 487-8501, Japan
[b] Department of Orthopaedic Surgery, Graduate School of Medicine, Kyoto University, 54 Kawahara-cho, Shogoin, Sakyo-ku, Kyoto 606-8507, Japan

ARTICLE INFO

Article history:
Received 22 October 2009
Received in revised form 6 January 2010
Accepted 7 January 2010
Available online 13 January 2010

Keywords:
Titanium
Calcium
Apatite
Scratch
Moisture

ABSTRACT

A calcium solution treatment was applied to a NaOH-treated titanium metal to give it bioactivity, scratch resistance and moisture resistance. The titanium metal was soaked in a 5 M NaOH solution and then a 100 mM $CaCl_2$ solution to incorporate Ca^{2+} ions into the titanium metal surface by ion exchange. This treated titanium metal was subsequently heated at 600 °C and soaked in hot water at 80 °C. The NaOH treatment incorporated ~5 at.% Na^+ ions into the Ti metal surface. These Na^+ ions were completely replaced by Ca^{2+} ions by the $CaCl_2$ treatment. The number of Ca^{2+} ions remained even after subsequent heat and water treatments. Although the NaOH–$CaCl_2$-treated titanium metal showed slightly higher apatite-forming ability in a simulated body fluid than the NaOH-treated titanium metal, it lost its apatite-forming ability during the heat treatment. However, subsequent water or autoclave treatment restored the apatite-forming ability of the NaOH–$CaCl_2$-heat-treated titanium metal. Although the apatite-forming ability of the NaOH-heat-treated titanium metal decreased dramatically when it was kept at high humidity, that of NaOH–$CaCl_2$-heat-water-treated titanium metal was maintained even in the humid environment. The heat treatment increased the critical scratch resistance of the surface layer of the NaOH–$CaCl_2$-treated titanium metal remarkably, and it did not deteriorate on subsequent water treatment.

1. Introduction

Titanium (Ti) metal and its alloys have been widely used in medical devices such as artificial joints and dental implants because of their high fracture toughness and good biocompatibility, however, they do not bond to living bone. It is desirable to provide a bone-bonding ability to Ti metal and its alloys. To achieve this, a technique was developed to coat Ti metal and its alloys with calcium phosphate using a plasma spray. However, this method cannot form an uniform bioactive layer on complex shapes, because only the surfaces exposed to the plasma are coated and calcium phosphate is liable to decompose in the living body.

Solutions and thermal treatments can form an uniform bioactive surface layer, even on complex shapes. It has been shown that Ti metal forms a sodium titanate layer on its surface when soaked in NaOH solution at 60 °C for 24 h and then heat treated at 600 °C for 1 h. Ti metal with a surface sodium titanate layer spontaneously forms a bone-like apatite on its surface in the body environment and directly bonds to living bone through this apatite layer [1–5]. These treatments were applied to the porous Ti metal layer of an artificial hip joint commercialized in Japan in 2007 [6]. However, the apatite-forming ability of NaOH- and heat-treated Ti metal is liable to decrease when the treated-Ti metal is stored in a humid environment for a long period of time, because of the release of Na^+ ions from the sodium titanate.

Ti metal containing Ca^{2+} ions on its surface, instead of Na^+ ions, is expected to exhibit a higher apatite-forming ability, since the released Ca^{2+} ions more effectively increase the ionic activity product of the apatite in the surrounding body fluid than released Na^+ ions [7]. However, calcium ions cannot be incorporated into the surface of Ti metal in the same manner as NaOH ions because of the low solubility of $Ca(OH)_2$ in water. Many studies on the incorporation of Ca^{2+} ions into Ti metal surfaces have been performed. Nayab et al. [8] reported that Ti metal with incorporated Ca^{2+} ions, incorporated using ion implantation, showed better cell adhesion properties than non-implanted Ti metal. However, implanted Ca^{2+} ions can reach only a shallow area, and the richest Ca^{2+} area exists a small distance below the top surface [9]. Sul [10] showed that about 11 at.% Ca ions were incorporated into a TiO_2 layer ~1300 nm thick on the surface of Ti metal by micro-arc oxidation in a calcium-containing mixed electrolyte system. The resultant dental implant showed a higher removal torque than untreated implant. However, this higher torque cannot be simply attributed to formation of a calcium-containing TiO_2 layer on the Ti metal, as a porous structure with a number of craters is formed on the

* Corresponding author. Tel.: +81 568 51 1111; fax: +81 568 51 5370.
E-mail address: t-kizuki@isc.chubu.ac.jp (T. Kizuki).

1742-7061/$ - see front matter © 2010 Acta Materialia Inc. Published by Elsevier Ltd. All rights reserved.
doi:10.1016/j.actbio.2010.01.007

surface of the Ti metal on micro-arc oxidation. Fröjd et al. [11] later reported that a calcium-incorporated titanium oxide layer formed on Ti metal by micro-arc oxidation gives greater bone contact than a calcium-free oxide layer. Song et al. [12] did not observe apatite formation in simulated body fluid (SBF) on a Ca-containing titanium oxide formed by micro-arc oxidation, but did so on a surface layer formed with amorphous $Ca(OH)_2$ by subsequent hydrothermal treatment with water at 250 °C for 2 h. Incorporation of calcium ions into Ti metal by hydrothermal treatment was also attempted by Nakagawa et al. [13]. They showed that a small number of calcium ions are incorporated into the surface of Ti metal by hydrothermal treatment with $CaCl_2$ solution at 200 °C for 24 h, and that thus treated Ti metal forms apatite on its surface in SBF. Park et al. [14] incorporated larger numbers of calcium ions into the surface of a Ti–6Al–4V alloy, by forming $CaTiO_3$ through hydrothermal treatment with NaOH and CaO solution at 180 °C for 24 h. The thus treated alloy also formed apatite on its surface in Hank's solution and showed an increased bone–implant contact. Ueda et al. [15] observed apatite formation in SBF on Ti metal which had first been treated with H_2O_2/HNO_3 solution at 80 °C for 60 min and then hydrothermally treated with $Ca(OH)_2$ solution at 180 °C for 12 h. Chen et al. [16] showed that calcium ions were incorporated into surface of porous Ti metal by hydrothermal treatment with 0.2 M $Ca(OH)_2$ solution at 250 °C for 8 h.

Both the micro-arc oxidation and hydrothermal treatments described above, however, need an apparatus specially designed to apply an electric field or high pressure to medical devices.

Raknagarm et al. [17] tried to incorporate calcium ions into the surface of Ti metal and its alloys by NaOH and $Ca(OH)_2$ solution treatments. Thus treated Ti metal and its alloy formed apatite on their surfaces in SBF. However, these metals were not heat treated after the NaOH and $Ca(OH)_2$ treatments. The resultant products showed neither high scratch resistance nor high apatite-forming ability.

This study attempted the preparation of Ti metal with a surface enriched with calcium ions by simple chemical and thermal treatments and examined the apatite-forming ability and scratch resistance of the resulting products, as well as stability of apatite-forming ability in humid environments.

2. Materials and methods

2.1. Sample preparation

Commercial pure Ti metal (Ti > 99.5%, Nilaco Co., Japan) $10 \times 10 \times 1$ mm^3 was polished with a No. 400 diamond disk and then washed in acetone, 2-propanol and ultrapure water with an ultrasonic cleaner for 30 min. The Ti metal was soaked in 5 ml of a 5 M NaOH solution at 60 °C for 24 h and then gently washed with ultrapure water. The NaOH-treated Ti metal was subsequently soaked in 10 ml of 100 mM $CaCl_2$ solution at 40 °C for 24 h and then gently washed with ultrapure water. The NaOH- and NaOH–$CaCl_2$-treated Ti metals were heated to 600 °C at a rate of 5 °C min^{-1} and at 600 °C for 1 h in an air atmosphere. The NaOH–$CaCl_2$-heat-treated Ti metal was subsequently subjected to hot water or autoclave treatment. For the hot water treatment the NaOH–$CaCl_2$-heat-treated Ti metal was soaked in 10 ml of ultrapure water at 80 °C for 24 h. For the autoclave treatment the NaOH–$CaCl_2$-heat-treated Ti metal was placed in an autoclave (SP300F, Yamato Scientific, Japan) at 121 °C for 0.5 h. The treated-Ti metals were gently washed with ultrapure water and then dried at 40 °C.

2.2. Surface characterization

Surface morphological changes of the Ti metal due to each treatment were observed by field emission scanning electron microscopy (FE-SEM) (S-4300, Hitachi, Japan). The surface compositions of the treated-Ti metals were measured by energy dispersive X-ray analysis (EDX) (EMAX-7000, Horiba, Japan). Three specimens were prepared for EDX measurement for each group and five points were analyzed for each specimen (total 15 points per group). Distributions of some elements near the surface of the treated-Ti metal were measured by Auger electron spectroscopy (AES) (PHI-670, ULVAC-PHI Inc., Japan). The surface phases of the treated-Ti metals were analyzed by thin film X-ray diffractometry (TF-XRD) (RINT2500, Rigaku Co., Japan) and Raman spectroscopy (LabRam HR800, Horiba Ltd., Japan).

The abrasion resistance of the surfaces of the treated-Ti metals were examined with a scratch tester (CSR-2000, Rhesca Co. Ltd., Japan). A diamond tip stylus 5 μm in diameter was used at a 200 g mm^{-1} spring rate to measure the critical scratch point of the surface layer. The amplitude, scratch speed and load rate were 100 μm, 10 μm s^{-1} and 100 mN min^{-1}, respectively, based on JIS R-3255. The mean values of critical scratch load were calculated from the measured values at six points for each group. The number of Ca^{2+} ions released from the treated-Ti metal by hot water treatment was measured by inductively coupled plasma atomic emission spectroscopy (ICP-AES) (SPS3100, SII NanoTechnology Inc., Japan).

2.3. Examination of apatite-forming ability

The apatite-forming abilities of Ti metals subjected to each treatment were examined in pH 7.40 SBF comprising 142.0 mM Na^+, 5.0 mM K^+, 1.5 mM Mg^{2+}, 2.5 mM Ca^{2+}, 147.8 mM Cl^-, 4.2 mM HCO_3^-, 1.0 mM HPO_4^{2-} and 0.5 mM SO_4^{2-}, approximately equal to those of human blood plasma at 36.5 °C. The SBF was prepared by dissolving reagent grade NaCl, $NaHCO_3$, KCl, $K_2HPO_4{\cdot}3H_2O$, $MgCl_2{\cdot}6H_2O$, $CaCl_2$ and Na_2SO_4 in ultrapure water, and buffering at pH 7.40 with tris(hydroxymethyl)aminomethane [$(CH_2OH)_3CNH_2$] and 1.0 M HCl aqueous solution at 36.5 °C [18]. After soaking in SBF for 1 day the samples were removed from the solution and washed with ultrapure water. The surfaces of the samples soaked in SBF were observed by FE-SEM.

2.4. Moisture resistance test

The treated-Ti metals were kept in a chamber that controlled the relative humidity at 95% at 80 °C for 1 week. They were soaked in SBF for 1 day and washed with ultrapure water. Their surfaces were observed by FE-SEM. Surface apatite formation was compared with that of the surfaces before being kept in the humidity chamber.

3. Results

Fig. 1 shows FE-SEM pictures of the Ti metal surfaces after various treatments. A fine network structure formed after NaOH treatment. This network structure was not essentially changed by subsequent treatments.

FE-SEM pictures of cross-sections of the Ti metal surface layers subjected to various treatments are shown in Fig. 2. A lath-like phase grew upward from the substrate after NaOH treatment and essentially did not change after subsequent treatments.

According to EDX analysis about 5 at.% of Na^+ ions were incorporated into the surface of the Ti metal after NaOH treatment, as shown in Table 1. These Na^+ ions were maintained even after heat treatment. The Na^+ ions incorporated into the Ti metal surface by the NaOH treatment were completely replaced by Ca^{2+} ions on subsequent $CaCl_2$ treatment. The number of Ca^{2+} ions was not changed by subsequent heat treatment, although it decreased slightly with

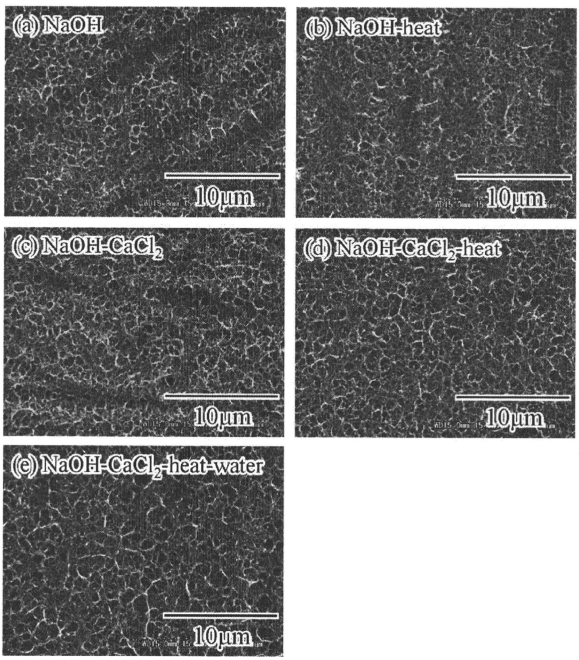

Fig. 1. FE-SEM photographs of the surfaces of Ti metals subjected to various treatments.

subsequent water treatment. The number of Ca^{2+} ions released into the water by hot water treatment was 0.15 ppm according to the ICP-AES measurements.

Depth profiles using Auger electron spectra of the Ti metal surfaces subjected to NaOH-heat and NaOH–$CaCl_2$-heat-water treatments are shown in Fig. 3. The concentration of Na^+ ions incorporated into the Ti metal surface decreased with increasing depth within 1 μm. The concentration of Ca^{2+} ions incorporated into the surface layer of the NaOH–$CaCl_2$-heat-water-treated Ti metal also decreased with increasing depth within about 1 μm. However, the calcium content at the top surface was a little lower than that at a depth of ~100 nm.

Figs. 4 and 5 show TF-XRD patterns and Raman spectra of the surface of Ti metals after various treatments. After the NaOH treatment sodium hydrogen titanate ($Na_xH_{2-x}Ti_3O_7{\cdot}nH_2O$) [19–21] was detected for the first time. Subsequent heat treatment transformed the sodium hydrogen titanate into sodium titanate ($Na_2Ti_6O_{13}$) [19–21] and rutile. The sodium hydrogen titanate was speculated to be isomorphously transformed into calcium hydrogen titanate by $CaCl_2$ treatment after NaOH treatment, since the $CaCl_2$ treatment changed neither the XRD patterns nor Raman spectra. The heat treatment transformed the calcium hydrogen titanate into a low crystalline calcium titanate and rutile. Subsequent water treatment did not change these phases.

The scratch resistances of the surface layers formed on Ti metal by various treatments are shown in Fig. 6. Ti metals treated with NaOH solution or NaOH and $CaCl_2$ solutions had a low scratch resistance, whereas those heat treated after chemical treatment had a remarkably high scratch resistance that did not decrease with subsequent water treatment. A significant difference in *t*-test was observed between the samples with heat treatment (NaOH-heat-, NaOH–$CaCl_2$-heat- and NaOH–$CaCl_2$-heat-water-treated Ti metals) and without heat treatment (NaOH- and NaOH–$CaCl_2$-treated Ti metals).

Fig. 7 shows FE-SEM photographs of the surfaces of the Ti metals soaked in SBF for 1 day after the various treatments. The depositions formed on the treated-Ti metal surfaces were assigned as apatite by TF-XRD. The NaOH-treated Ti metal showed relatively low apatite-forming ability in SBF, however, the apatite-forming ability increased remarkably on subsequent heat treatment. The NaOH–$CaCl_2$-treated Ti metal showed a slightly higher apatite-forming ability than the NaOH-treated Ti metal. Its apatite-forming ability decreased significantly with subsequent heat treatment, but increased remarkably after hot water or autoclave treatment following heat treatment. The Ca/P ratios of the apatite formed on the NaOH–$CaCl_2$-heat-water-treated Ti metal was found to be 1.62 by EDX analysis. It was no different from that of the apatite formed on NaOH-heat-treated Ti metal.

It lost apatite-forming ability, also when it was stored at room temperature in air atmosphere for 2 month. However, it did not decrease apatite-forming ability when it was kept at 80 °C in air atmosphere for 1 week. Fig. 8 shows FE-SEM pictures of the surface of the NaOH-heat-treated and NaOH–$CaCl_2$-heat-water-treated Ti metals which were soaked in SBF for 1 day after being kept at

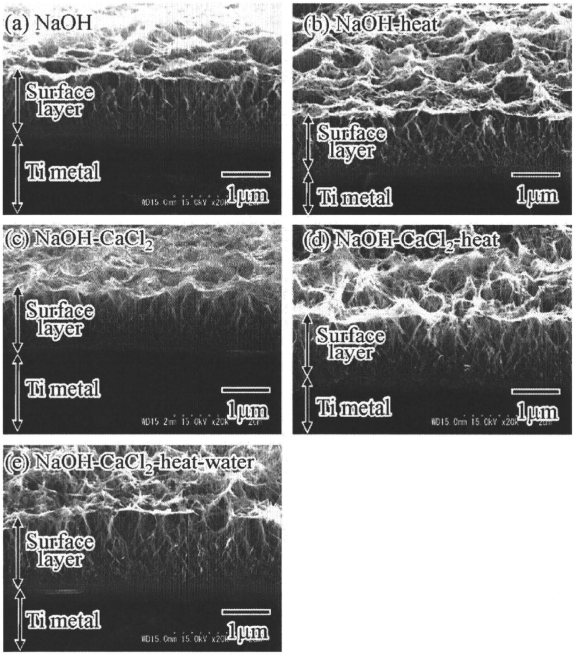

Fig. 2. FE-SEM photographs of cross-sections of Ti metals subjected to various treatments.

Table 1
Element concentration measured by EDX at surfaces of Ti metals subjected to various treatments.

Treatment	Element/at.%				
	Ti	O	C	Na	Ca
NaOH	26.5	62.5	5.8	5.3	0
(std. dev.)	(0.2)	(0.3)	(0.2)	(03)	(0)
NaOH-heat	25.9	65.1	3.5	5.6	0
(std. dev.)	(0.7)	(0.2)	(0.2)	(0.5)	(0)
NaOH–$CaCl_2$	25.0	64.2	6.7	0	4.1
(std. dev.)	(0.2)	(0.3)	(0.3)	(0)	(0.1)
NaOH–$CaCl_2$-heat	25.9	65.0	4.9	0	4.1
(std. dev.)	(0.4)	(0.2)	(0.2)	(0)	(0.2)
NaOH–$CaCl_2$-heat-water	25.4	65.1	5.8	0	3.7
(std. dev.)	(0.3)	(0.5)	(0.2)	(0)	(0.1)

95% relative humidity at 80 °C for 1 week as a moisture resistance test. Apatite formation was not observed on the surface of the NaOH-heat-treated Ti metal after the moisture resistance test, whereas it was fully observed on NaOH–$CaCl_2$-heat-water-treated Ti metal even after the moisture resistance test.

About 30% of the Na^+ ions at the surface of the NaOH-heat-treated Ti metal were lost because of the moisture resistance test, whereas the number of Ca^{2+} ions at the surface of NaOH–$CaCl_2$-heat-water-treated Ti metal did not change even after the moisture resistance test, as shown in Table 2. No structural change was observed in TF-XRD patterns of the NaOH-heat-treated and NaOH–$CaCl_2$-heat-water-treated Ti metals after the moisture resistance test.

4. Discussion

It is apparent from the experimented results that a fairly large number of calcium ions were easily incorporated into the surface of Ti metals when first treated with a NaOH solution and then soaked in a $CaCl_2$ solution (Table 1 and Fig. 3). This is because the sodium hydrogen titanate ($Na_2H_{2-x}Ti_3O_7{\cdot}nH_2O$) that formed on the Ti metal surface during the first NaOH treatment has a layered structure [19] and the Na^+ ions in it were easily replaced by Ca^{2+} ions on $CaCl_2$ treatment (Fig. 4). However, the resultant Ti metal enriched with calcium ions on its surface showed only a slightly higher apatite-forming ability in SBF than NaOH-treated Ti metal (Fig. 7c) and had a low scratch resistance (Fig. 6). When heat treated at 600 °C, however, the resultant product had a high scratch resistance (Fig. 6), but showed extremely low apatite-forming ability (Fig. 7d). This might be attributed to the low mobility of the Ca^{2+} ions in the calcium titanate formed from calcium hydrogen titanate by heat treatment (Fig. 4). The apatite-forming ability of heat-treated Ti metal increased remarkably when it was subsequently treated with hot water or by autoclaving (Fig. 7e and f). This might be attributed to the increased mobility of Ca^{2+} ions in the calcium titanate due to the water or autoclave treatment. Table 1, Fig. 3 and ICP-AES measurements showed that a small number of Ca^{2+} ions at the surface of the treated-Ti metal were released